Impact of carotid bifurcation geometry on atherosclerotic formation: A hemodynamic study

Xin-Ke Yao[1†*], Yan Cai[1†], Jie Gao[2†], Ge-Lin Xu[2‡], Zhi-Yong Li[1,3‡]

[1]School of Biological Science & Medical Engineering, Southeast University, Nanjing 210096, P.R. China
[2]Department of Neurology, Jinling Hospital, Medical School of Nanjing University, Nanjing 210002, P.R. China
[3]School of Chemistry, Physics and Mechanical Engineering, Queensland University of Technology, Brisbane, QLD 4001, Australia

*Presenting author: yaofe6881@sina.cn

† These authors contributed equally to this article.

[‡]Corresponding author: gelinxu@nju.edu.cn; zylicam@gmail.com

Abstract:

Background: Recent studies have demonstrated major variations in carotid bifurcation geometry, in favor of the concept that individual vascular anatomy may play a role in the development of atherosclerosis. To test these assumptions, the present study aimed to investigate the impact of wide variations on carotid artery hemodynamics by computational fluid dynamic (CFD) simulations.
Method: In the present work, six groups of three-dimensional synthetic models of carotid bifurcation with different morphological parameters were established by ANSYS. The geometric variations included internal carotid artery (ICA) /common carotid artery (CCA) diameter ratio, sinus/CCA diameter ratio, external carotid artery (ECA)/CCA diameter ratio, ICA angle, tortuosity and planarity. Pulsatile blood flow through a model of the carotid artery bifurcation was simulated using a finite volume numerical method. The changes of inlet velocity during the cardiac cycle were taken into consideration while outlet pressure was a constant value. The simulated results were visualized in TECPLOT for subsequent analysis.
Result: The temporal average value of wall shear stress (AWSS) on the sinus wall was obtained from the hemodynamic simulations. Multiple regression analysis revealed a significant ($P<0.001$) relationship between AWSS and both ICA angle ($\beta=0.48$) and sinus/CCA diameter ratio ($\beta=-0.48$). Larger ICA angles generally increase the AWSS on the sinus wall, hence lowering the risk of plaque build-up. In contrast, high sinus/CCA diameter ratio was found to decrease AWSS on the sinus for geometries with the baseline ICA angle.
Conclusion: Compared to benchmark model, the changes of carotid bifurcation geometry can lead to apparent differences in hemodynamics. It may therefore be reasonable to consider certain geometric features to be surrogate markers of low AWSS, which is mainly related to atherosclerotic formation.
Keywords: Atherosclerosis, Hemodynamics, Carotid Bifurcation, Wall Shear Stress.

Introduction

As one of the most dangerous diseases, atherosclerosis of large arteries causes one fourth of stroke cases worldwide [1]. Atherosclerotic plaques are prone to appearing near arterial bifurcations and bends, which leads to an acknowledged concept that the unique vascular anatomy of each person plays an important role in the development of this disease. The ability to understand the underlying mechanism of geometry effects in atherosclerotic plaque formation would be of great clinical value for patient prognosis [2]- [3].

While there is some controversy over the most indicative geometry markers related to the hemodynamic environment and subsequent atherosclerosis formation, many clinical studies strongly suggest the relationship between geometry of carotid bifurcation and disturbed flow. Lee et al. [4] modeled 50 carotid bifurcation geometries derived from magnetic resonance imaging (MRI) of 25 young adults and found that disturbed flow is sensitive to both proximal area ratio and bifurcation tortuosity. Markl et al. [5] analyzed the in vivo distribution of absolute WSS in the carotid bifurcation to evaluate its dependence on geometry. Time-resolved 3D blood flow in this research was achieved with flow-sensitive 4D MRI in 64 normal carotid bifurcations and 17 carotid arteries with moderate stenosis. Common to these studies is the assumption that secondary effects of stenosis on geometry can be ignored. To systematically examine the influence of geometry on the blood flow pattern, a Y-shaped model was established by Nguyen et al. to quantify the risk of atherogenesis associated with different bifurcation angle and the out-of-plane angle. However, they excluded many other geometry factors, such as the diameter ratios and tortuosity.

The objective of this work is to test the impact of wide variations of carotid bifurcation geometry on hemodynamics by control variate method. Six geometric variations, including internal carotid artery（ICA）/common carotid artery (CCA) diameter ratio, sinus/CCA diameter ratio, external carotid artery (ECA)/CCA diameter ratio, ICA angle, tortuosity and planarity, , are designed to establish 30 synthetic models. Computational fluid dynamic (CFD) simulations are performed with the same initial and boundary conditions. The numerical results of flow patterns and wall shear stress (WSS) on the sinus wall are compared between different synthetic models. In addition, the significance analysis is carried out between the temporal average value of wall shear stress (AWSS) and certain geometric variations.

Materials and Method

Geometry of the models

The human CCA bifurcates into the ECA and the ICA at approximately the level of the fourth cervical vertebra. Bharadvaj et al. [6] digitized film angiograms of patients to develop the Y-shaped model of the average human carotid bifurcation (Y-AHCB), which then has been widely used in experimental and numerical investigations of hemodynamics in the carotid bifurcation [7]- [13]. However, much arteriograms and specimen figures revealed the fact that most ICA is bent inward [14]- [16]. To optimize it, the tuning-fork-sharped model of average human carotid bifurcation (TF-AHCB) was proposed by observation and statistical analysis of specimens from 74 cadavers [17]. In the present study, the benchmark model was established according to the TF-shaped model (Figure 1).

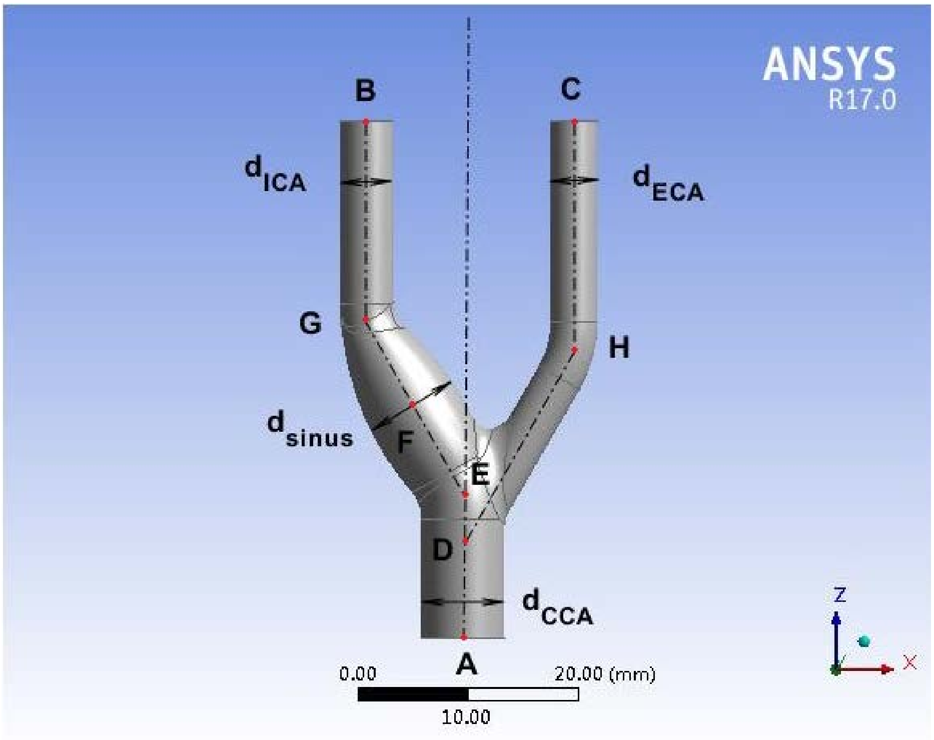

Figure 1. Typical carotid artery geometry of the benchmark model (the tuning-fork-sharped model of average human carotid bifurcation, TF-AHCB model).

The geometric values of the benchmark model are presented in Table 1. Specifically, the arteries were modeled by cylindrical pipes through the operation of sweep. A specific graphics revolved around the center line of ICA to form the sinus region. The CCA was modeled by a cylinder with length of 13mm. The ICA outlet and ECA outlet were at the same horizontal plane in benchmark model. That is, both ICA and ECA outlet had a perpendicular distance of 47mm to CCA inlet. The diameter of ICA was 4.87mm while ECA had a diameter of 4.27mm. The carotid sinus, whose maximum diameter was 8.60mm, had the same center line as the ICA. The maximum cross section of sinus intersected the center line at F, which was the midpoint of sinus axis. In order to smooth the interface, a fixed radius blend of 3mm was applied in present work.

The ICA angle was defined as the angle between the center line of sinus and of CCA, while planarity angle was defined as the angle of the ICA with the CCA-ECA plane. The ratio between the diameter of distal ICA and CCA was called ICA/CCA diameter ratio. Similarly, the ratio between the diameter of distal ECA and CCA was called ECA/CCA diameter ratio. Sinus/CCA diameter ratio was calculated as the maximum diameter of ICA sinus divided by CCA diameter. Although vessel tortuosity was usually defined as a ratio between Euclidean distance and the length of the centerline, it was represented as the angle between the axis of distal ICA and sinus in this study. Hence, larger tortuosity angle means straighter ICA.

Table 1. Dimensions of the benchmark model (mm)

CCA			ICA				ECA		
AD	AE	d_{CCA}	EG	GB	d_{sinus}	d_{ICA}	DH	HC	d_{ECA}
8.5	13	7.58	17.486	18.856	8.60	4.87	18.205	21	4.27

Diameter ratios varied based on the measurements taken by Ding et al, where unit dimensions of ICA, ECA, sinus and CCA diameter have been discussed. According to the data list in Table 1, the baseline ICA/CCA, sinus/CCA, ECA/CCA diameter ratio (0.64, 1.13, and 0.56, respectively) can be calculated. The average bifurcation angle was 63.6° in a control group of older subjects presented by Thomas et al. [18]. Therefore, the baseline ICA angle and ECA angle were both 30° in current study. Because distal ICA was parallel to CCA and distal ECA in benchmark model, baseline tortuosity angle was doubtlessly 150°. The variation of ICA angle ranged from 10° to 50° and tortuosity angle from 120° to 160°. In addition, planarity angle was varied from 0 to 10° based on the discovery that the average off-plane angle was 7.0° for young adults versus 8.5° for another age group.

Computational fluid dynamics

Tetrahedral-element meshes were generated by ICEM CFD, Version 17.0 (ANSYS Inc.) using a maximum element size of 0.5mm and a minimum size of 0.2mm, which was demonstrated to be sufficient for resolving WSS [19].

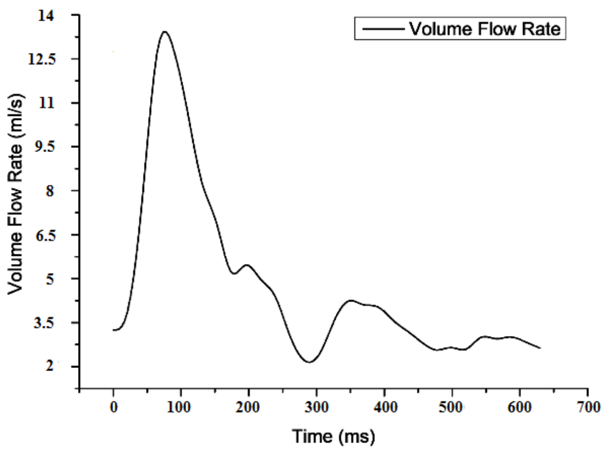

Figure 2. Inlet volume flow rate in one cardiac cycle

Blood was assumed to be a Newtonian fluid in large blood vessels as the size of blood cells there is small compared to the diameter of the tubes [20]. The viscosity of blood is approximately four times that of water and its density ranges from 1020 to 1150 kg/m^3. Therefore, blood was modeled to have a density of 1056 kg/m^3 and a viscosity of 0.0035 Pa·s in present work. The vessel wall was assumed to be rigid without displacement.

The CCA inflow boundary condition was a time-dependent volume flow waveform of a healthy volunteer (Figure 2). According to the inlet volume flow rate, the mean blood velocity at the inlet can be obtained by following equation:

$$v_{maen}(t) = \frac{q(t)}{\pi(\frac{d}{2})^2} \tag{1}$$

where d is the diameter of the inlet, t is time, q is the volume flow rate and v_{mean} is the mean velocity. The pressure at the ICA and ECA outlets was set to be equal to 75mmHg. Transient CFD simulation was processed with Fluent, Version 17.0 (ANSYS Inc.) for one cardiac cycles with a time step of 0.00628 seconds. In the CFD simulation, the convergence criterion was satisfied when the residual of continuity was less than 10^{-4}.

The main hemodynamic parameter studied in present work was AWSS. It was defined as:

$$\mathrm{AWSS} = \left|\frac{1}{T}\int_0^T \overrightarrow{WSS}\, dt\right| \tag{2}$$

Additionally, the median values of parameter were used for further analysis. The hemodynamic results were obtained by Fluent and Tecplot 360, Version 2014 (Tecplot Inc.).

Multiple linear regression was used to quantify the relationship between AWSS and predictor variables. The overall quality of the regression was assessed by Pearson's correlation coefficient, adjusted by the number of independent predictors (R_{adj}^2). The relative contributions of the geometric variables were identified by the standardized regression coefficients (β). Statistical analyses were carried out by SPSS 19.0.

Results

Simulations and analysis were performed for a wide range of diameter ration and angles. The changes of instantaneous WSS at systolic peak with different geometry were shown in Figure 3. The region indicated by dark blue color has WSS lower than the critical value of 0.4 Pa [21] while red color represents WSS larger than 15 Pa. The dark blue region only appears on the outer wall of the carotid sinus, which indicates the low WSS on the sinus wall as a stimulative factor of intima-media thickness. Furthermore, the WSS is lower at the entry of sinus and higher at the exit of sinus. There is a red region at the terminal of the sinus in all synthetic models. When the ICA/CCA diameter ratio increases, this red region becomes contractible most dramatically.

To analyze the relationship of AWSS and geometry variations more directly, we perform the curves of the median of sinus AWSS in different synthetic models (Figure 4). The median of sinus AWSS changes linearly according to the parameters. It decreased when sinus/CCA and ECA/CCA diameter ratio increased. In contrast, the rise of ICA/CCA diameter ratio can lead to high AWSS on the sinus wall, which indicated the hindering effect of narrow downstream. AWSS increased with the enlargement of ICA angle. This trend became gentle gradually when

ICA/CCA=0.54 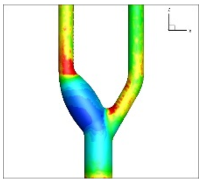	**ICA/CCA=0.59** 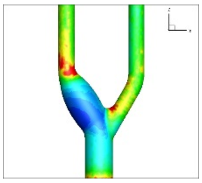	**ICA/CCA=0.64** 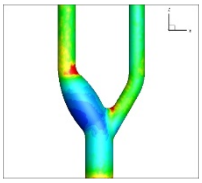	**ICA/CCA=0.69** 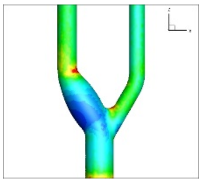	**ICA/CCA=0.74** 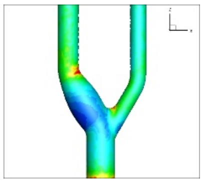
Sinus/CCA=1.03 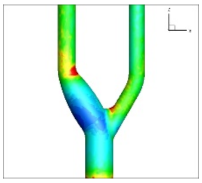	**Sinus/CCA=1.08** 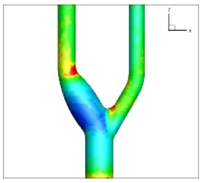	**Sinus/CCA=1.13** 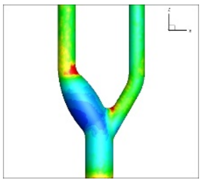	**Sinus/CCA=1.18** 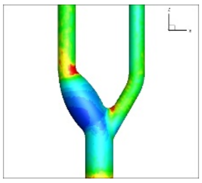	**Sinus/CCA=1.23** 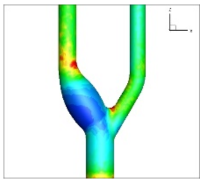
ECA/CCA=0.46 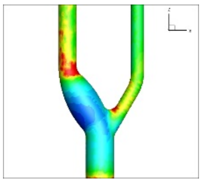	**ECA/CCA=0.51** 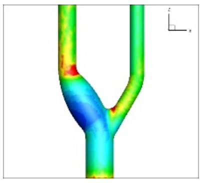	**ECA/CCA=0.56** 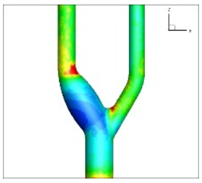	**ECA/CCA=0.61** 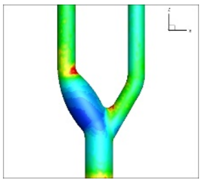	**ECA/CCA=0.66** 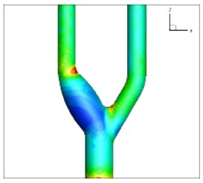
ICA angle=10 ° 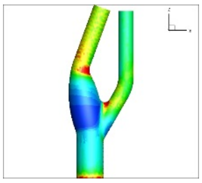	**ICA angle=20 °** 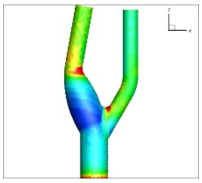	**ICA angle=30 °** 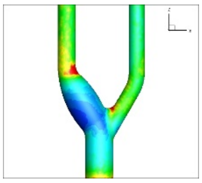	**ICA angle=40 °** 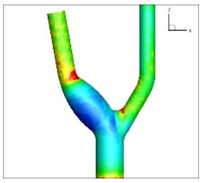	**ICA angle=50 °** 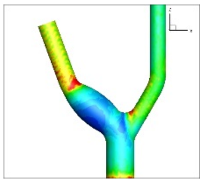
Tortuosity=120 ° 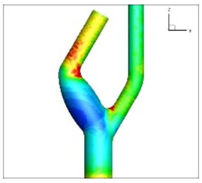	**Tortuosity=130 °** 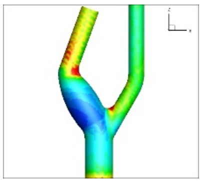	**Tortuosity=140 °** 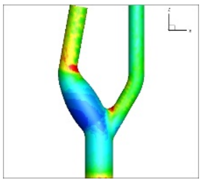	**Tortuosity=150 °** 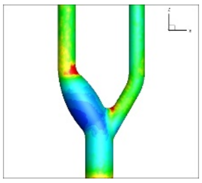	**Tortuosity=160 °** 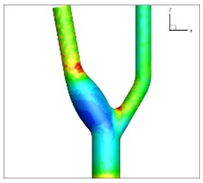
Planarity=0 ° 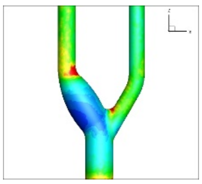	**Planarity=2.5 °** 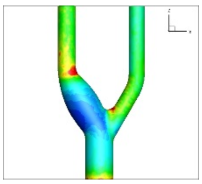	**Planarity=5 °** 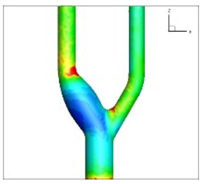	**Planarity=7.5 °** 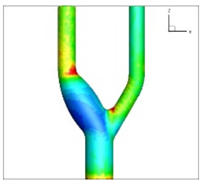	**Planarity=10 °** 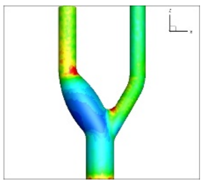

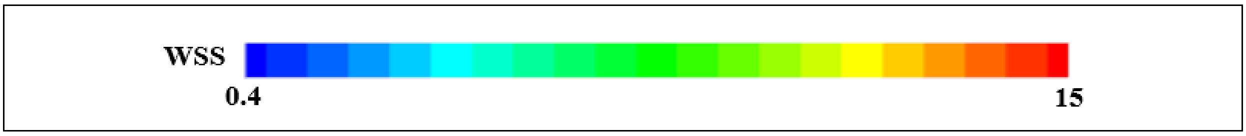

Figure 3. WSS at systolic peak with different geometry

ICA angle was larger than 30°. Tortuosity angle had a similar effect on AWSS. While it should be noticed that the larger tortuosity angle was, the straighter the ICA was. Hence, bent ICA was more liable to have plaques on the sinus wall. With the baseline ICA angle of 30°, higher off-plane angle results in lower AWSS, which was consistent with the notion suggested by Nguyen et al. [22] previously that planarity angle is a major contributor to vascular disease when ICA angle is larger than 25°.

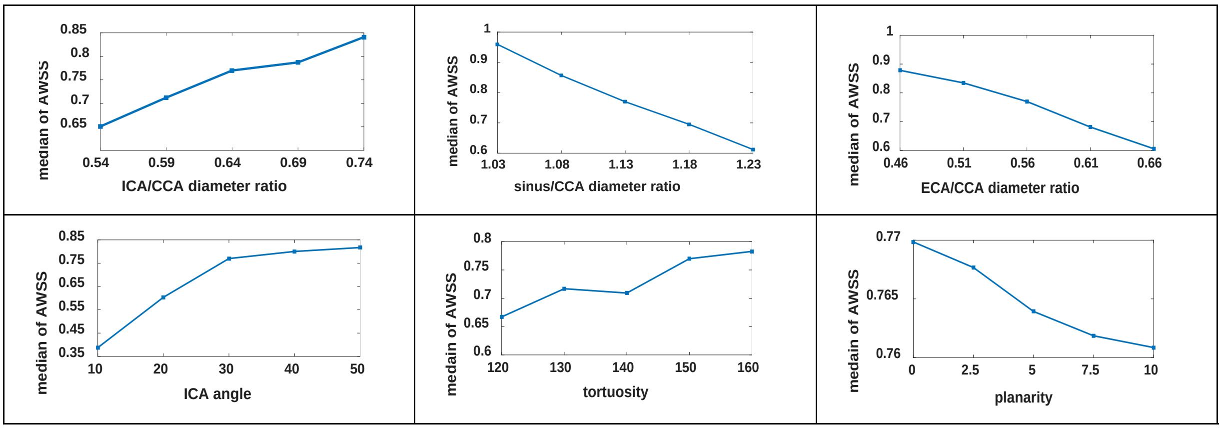

Figure 4. The relationship between AWSS and geometrical variations

Table 2. Multiple linear regressions of AWSS on the sinus wall with geometric variations

		Median of AWSS
Model Quality	R^2_{adj}	0.634
	P	<0.001
ICA/CCA Diameter Ratio	β	0.254
	P	0.030
Sinus/CCA Diameter Ratio	β	-0.478
	P	<0.001
ECA/CCA Diameter Ratio	β	-0.389
	P	0.002
ICA Angle	β	0.483
	P	<0.001
Tortuosity	β	0.147
	P	0.197

Planarity	β	0.072
	P	0.552

As plaque would preferentially form around the carotid artery bifurcation (extracranial site) and the carotid artery siphon (intracranial site), carotid sinus was chosen as the particular area to be analyzed. As summarized in Table 2, multiple regressions revealed that the combination of ICA angle and sinus/CCA diameter ratio may be far stronger predictors of AWSS on the sinus wall (P<0.001). However, β for tortuosity and planarity was not significant (P>0.1). The median of AWSS had a positive correlation with ICA angle (β=0.483) and a negative correlation with sinus/CCA diameter ratio (β=-0.478).

Discussion

It is acknowledged that an individual's vascular anatomy or local hemodynamics will affect the progression of atherosclerosis disease. Most studies were carried out to explore the impact of geometry on stenosis through patient-derived carotid arteries. Thomas et al. [18] researched on 25 young adults and 25 older subjects and pointed out that there is a complex interrelationship among vascular geometry, local hemodynamics, vascular aging, and atherosclerosis. Interindividual variations of carotid bifurcations rise dramatically due to aging or early atherosclerosis. Besides, 178 samples were analysed by Phan et al. [23] to demonstrate that carotid anatomy and geometry, such as ICA angle and ICA radius at the bifurcation, may enhance the risk of stenosis independent of traditional vascular risk factors like age and smoker. Multiple factors will change simultaneously in individual carotid arteries. To examine the effects of each variation systematically, six groups of ideal models with different morphologic parameters were established in this study. There is only one variation changing in each group. The present investigation has demonstrated wide geometric variations in the exposure to low WSS.

It is noteworthy that low WSS was invariably focal on the sinus wall in all synthetic models. Studied of hemodynamics have demonstrated that the pulsatile ‘‘disturbed’’ flow (with low and oscillating shear stress) patterns are one of the dominant flow features for atherosclerosis formation [24]. Therefore, there is no doubt that the risk of atherosclerotic disease is directly associated with the low WSS region on the carotid sinus. The median value of AWSS on the particular portion of sinus wall was calculated to evaluate the sinus hemodynamic level in this study. It was found that the main factors leading to atherosclerosis formation were ICA angle and sinus/CCA diameter ratio [25]. The important role for branch angle has been suggested in previous model studies [26], which is consistent with our finding here. Moreover, Karino and Goldsmith [25] insisted the relative importance of diameter ratio versus angle on vortex formation by calculating a T-junctions model with wide variations.

As mentioned in Methods, a few assumptions were made to simplify the analysis. For example, the arterial wall was considered as a rigid one with no slip which was contrary to the elasticity of human vessels. Moreover, flow entering the vasculature after passing a straight tube with a cross sectional area the same as inlet region will lead to a fully-developed entry flow different from reality. These limitations make it reasonable to believe that only a minor effect on the resulting carotid bifurcation flow dynamics has been analysed in current study.

Aside from the modeling assumptions, a major shortcoming was the deficiency of other hemodynamic parameters. The present work concentrated on the WSS distribution of the carotid arteries. The impact of wall shear stress gradient (WSSG) and oscillatory shear index (OSI) on atherosclerosis formation was ignored. The continued perfection of hemodynamic analysis will be performed in further study.

The following directions may be further investigated in the future. First, more 3-dimensional geometric parameters can be analysed. Most morphologic variations suggested in present work, such as diameter ratio, angle and even tortuosity, were confined to 2-dimensional space which is incongruent with realistic carotid bifurcation anatomy. Then, patient-specific models based on imaging of carotid artery will be attached to verify the consequence of current study. In addition, significant displacement caused by blood flow should be taken into consideration in CFD simulation. The elasticity of arterial wall, in turn, will make a difference in flow pattern. This interaction can be coupled in future study.

Conclusion

In summary, the present study investigated the impact of wide variations on carotid artery hemodynamics by computational fluid dynamic (CFD) simulations. Geometric variation, including diameter ratio, ICA angle, tortuosity and planarity, can result in significant changes of WSS distribution. Among them, ICA angle and sinus/CCA diameter ratio were most relevant with AWSS on the sinus wall. That is, these two parameters had remarkable effect on plaque formation. The certain geometric features suggested in this work, in the sense, can be used as surrogate markers of low AWSS, and even as predictors of atherosclerotic formation.

Acknowledgements

This research is supported by the National Basic Research Program of China (973 program) (No. 2013CB733800), the National Nature Science Foundation of China (No. 11422222, 11302050, 81571143), the Fundamental Research Funds for the Central Universities, the National Demonstration Center for Experimental Biomedical Engineering Education (Southeast University), and ARC (FT140101152).

References

[1] Ruan, L., Chen, W., Srinivasan, S. R., Sun, M., Wang, H., Toprak, A., & Berenson, G. S. (2009). Correlates of common carotid artery lumen diameter in black and white younger adults. *Stroke*, *40*(3), 702-707.

[2] Ku, D. N., Giddens, D. P., Zarins, C. K., & Glagov, S. (1985). Pulsatile flow and atherosclerosis in the human carotid bifurcation. Positive correlation between plaque location and low oscillating shear stress. *Arteriosclerosis, thrombosis, and vascular biology*, *5*(3), 293-302.

[3] Younis, H. F., Kaazempur-Mofrad, M. R., Chan, R. C., Isasi, A. G., Hinton, D. P., Chau, A. H., ... & Kamm, R. D. (2004). Hemodynamics and wall mechanics in human carotid bifurcation and its consequences for atherogenesis: investigation of inter-individual variation. *Biomechanics and modeling in mechanobiology*, *3*(1), 17-32.

[4] Lee, S. W., Antiga, L., Spence, J. D., & Steinman, D. A. (2008). Geometry of the carotid bifurcation predicts its exposure to disturbed flow. *Stroke*,*39*(8), 2341-2347.

[5] Markl, M., Wegent, F., Zech, T., Bauer, S., Strecker, C., Schumacher, M., ... & Harloff, A. (2010). In vivo wall shear stress distribution in the carotid artery.*Circulation: Cardiovascular Imaging*, *3*(6), 647-655.

[6] Bharadvaj, B. K., Mabon, R. F., & Giddens, D. P. (1982). Steady flow in a model of the human carotid bifurcation. Part I—flow visualization. *Journal of biomechanics*, *15*(5), 349-362.

[7] Perktold, K., Resch, M., & Florian, H. (1991). Pulsatile non-Newtonian flow characteristics in a three-dimensional human carotid bifurcation model. *J Biomech Eng*, *113*(4), 464-475.

[8] Perktold, K., Thurner, E., & Kenner, T. (1994). Flow and stress characteristics in rigid walled and compliant carotid artery bifurcation models.*Medical and Biological Engineering and Computing*, *32*(1), 19-26.

[9] Perktold, K., & Rappitsch, G. (1995). Computer simulation of local blood flow and vessel mechanics in a compliant carotid artery bifurcation model. *Journal of biomechanics*, *28*(7), 845-856.

[10] Lee, D., & Chiu, J. J. (1996). Intimal thickening under shear in a carotid bifurcation—a numerical study. *Journal of biomechanics*, *29*(1), 1-11.

[11] Gijsen, F. J. H., Palmen, D. E. M., Van der Beek, M. H. E., Van de Vosse, F. N., Van Dongen, M. E. H., & Janssen, J. D. (1996). Analysis of the axial flow field in stenosed carotid artery bifurcation models—LDA experiments. *Journal of biomechanics*, *29*(11), 1483-1489.

[12] Rindt, C. C. M., & Steenhoven, A. V. (1996). Unsteady flow in a rigid 3-D model of the carotid artery bifurcation. *TRANSACTIONS-AMERICAN SOCIETY OF MECHANICAL ENGINEERS JOURNAL OF BIOMECHANICAL ENGINEERING*, *118*, 90-96.

[13] Ma, P., Li, X., & Ku, D. N. (1997). Convective mass transfer at the carotid bifurcation. *Journal of biomechanics*, *30*(6), 565-571.

[14] DeBakey, M. E., Lawrie, G. M., & Glaeser, D. H. (1985). Patterns of atherosclerosis and their surgical significance. *Annals of surgery*, *201*(2), 115.

[15] Salzar, R. S., Thubrikar, M. J., & Eppink, R. T. (1995). Pressure-induced mechanical stress in the carotid artery bifurcation: a possible correlation to atherosclerosis. *Journal of biomechanics*, *28*(11), 1333-1340.

[16] Nicholls, S. C., Phillips, D. J., Primozich, J. F., Lawrence, R. L., Kohler, T. R., Rudd, T. G., & Strandness, D. E. (1989). Diagnostic significance of flow separation in the carotid bulb. *Stroke*, *20*(2), 175-182.

[17] Ding, Z., Wang, K., Li, J., & Cong, X. (2001). Flow field and oscillatory shear stress in a tuning-fork-shaped model of the average human carotid bifurcation. *Journal of Biomechanics*, *34*(12), 1555-1562.

[18] Thomas, J. B., Antiga, L., Che, S. L., Milner, J. S., Steinman, D. A. H., Spence, J. D., ... & Steinman, D. A. (2005). Variation in the carotid bifurcation geometry of young versus older adults. *Stroke*, *36*(11), 2450-2456.

[19] Moyle, K. R., Antiga, L., & Steinman, D. A. (2006). Inlet conditions for image-based CFD models of the carotid bifurcation: is it reasonable to assume fully developed flow?. *Journal of biomechanical engineering*, *128*(3), 371-379.

[20] Ku, D. N. (1997). Blood flow in arteries. *Annual review of fluid mechanics*,*29*(1), 399-434.

[21] Malek, A. M., Alper, S. L., & Izumo, S. (1999). Hemodynamic shear stress and its role in atherosclerosis. *Jama*, *282*(21), 2035-2042.

[22] Phan, T. G., Beare, R. J., Jolley, D., Das, G., Ren, M., Wong, K., ... & Srikanth, V. (2012). Carotid artery anatomy and geometry as risk factors for carotid atherosclerotic disease. Stroke, 43(6), 1596-1601.

[23] Nguyen, K. T., Clark, C. D., Chancellor, T. J., & Papavassiliou, D. V. (2008). Carotid geometry effects on blood flow and on risk for vascular disease. *Journal of biomechanics*, *41*(1), 11-19.

[24] Ku, D. N., & Giddens, D. P. (1983). Pulsatile flow in a model carotid bifurcation. *Arteriosclerosis, Thrombosis, and Vascular Biology*, *3*(1), 31-39.

[25] Karino, T., Kwong, H. H., & Goldsmith, H. L. (1979). Particle flow behaviour in models of branching vessels: I. Vortices in 90 degrees T-junctions.*Biorheology*, *16*(3), 231-248.

[26] Friedman, M. H., O'brien, V., & Ehrlich, L. W. (1975). Calculations of pulsatile flow through a branch: implications for the hemodynamics of atherogenesis. *Circulation Research*, *36*(2), 277-285.